IVYSPRING
INTERNATIONAL PUBLISHER

Theranostics

Research Paper

Coronary Serum Exosomes Derived from Patients with Myocardial Ischemia Regulate Angiogenesis through the miR-939-mediated Nitric Oxide Signaling Pathway

Hao Li[1*], Yiteng Liao[1*], Lei Gao[2], Tao Zhuang[2], Zheyong Huang[3], Hongming Zhu[2✉], Junbo Ge[1,3✉]

1. Department of Cardiology, Shanghai Tenth People's Hospital, Tongji University School of Medicine, Shanghai 200072, China.
2. Translational Medical Center for Stem Cell Therapy & Institute for Regenerative Medicine, Shanghai East Hospital, Tongji University School of Medicine, Shanghai 200120, China.
3. Department of Cardiology, Shanghai Institute of Cardiovascular Diseases, Zhongshan Hospital, Fudan University, Shanghai 200032, China.

*Hao Li and Yiteng Liao contributed equally to this work.

✉ Corresponding authors: Hongming Zhu: zhm@tongji.edu.cn and Junbo Ge: junboge@hotmail.com

Abstract

Rationale: Angiogenesis is a crucial step towards tissue repair and regeneration after ischemia. The role of circulating exosomes in angiogenic signal transduction has not been well elucidated. Thus, this study aims to investigate the effects of coronary serum exosomes from patients with myocardial ischemia on angiogenesis and to elucidate the underlying mechanisms.

Methods and Results: The patients were enrolled according to the inclusion and exclusion criteria. Coronary blood was obtained from the angiography catheter. Serum exosomes were purified and characterized by their specific morphology and surface markers. *In vitro* analysis showed that compared to exosomes from healthy controls (con-Exo), exosomes from patients with myocardial ischemia (isc-Exo) enhanced endothelial cell proliferation, migration and tube formation. In a mouse hind-limb ischemia model, blood perfusion and histological staining demonstrated that isc-Exo significantly promoted blood flow recovery and enhanced neovascularization compared to con-Exo. Further, we revealed that cardiomyocytes, but not cardiac fibroblasts or endothelial cells, were initiated to release exosomes under ischemic stress; cardiomyocytes might be the source of bioactive exosomes in coronary serum. In addition, microarray analysis indicated that miR-939-5p was significantly down-regulated in isc-Exo. By knockdown and overexpression analyses, we found that miR-939-5p regulated angiogenesis by targeting iNOS. miR-939-5p inhibited both iNOS's expression and its activity, attenuated endothelial NO production, and eventually impaired angiogenesis.

Conclusions: Exosomes derived from patients with myocardial ischemia promote angiogenesis via the miR-939-iNOS-NO pathway. Our study highlights that coronary serum exosomes serve as an important angiogenic messenger in patients suffering from myocardial ischemia.

Key words: exosomes, myocardial ischemia, angiogenesis, miR-939-5p

Introduction

Ischemic heart disease is the leading health concern all over the world which is responsible for about 8.2 million deaths and many more heart failures globally each year, leaving a heavy economic burden [1]. Although percutaneous coronary intervention can largely restore coronary perfusion after acute myocardial infarction (MI), it is powerless to rebuild the damaged microvascular architecture in ischemic myocardium. Since angiogenesis is a crucial step towards tissue repair and regeneration after ischemia,

exploring the angiogenic mechanism has long been a holy grail of cardiovascular research.

Recently, a growing number of studies have suggested the key role of cell-to-cell communication in cardiac remodeling post MI. The surviving cardiac cells try to communicate with nearby or distant cells by sending warning or regulatory signals in order to maintain homeostasis and promote cardiac repair [2]. Exosomes are a group of newly defined extracellular vesicles and are characterized by their size, markers and origin [3]. They are typically 30-100 nm in size and contain specific surface markers like CD9, CD63 and flotillin. They are produced by inward budding of the cytoplasmic multivesicular bodies and released by the fusion of the multivesicular body and cell membrane [3]. Accumulating evidence have demonstrated the important functions of exosomes in cell-cell communications: exosomes can act as cargos to deliver specific nucleic acids and proteins to the target cells and eventually regulate the phenotype of host cells [4-7]. Recently, stress-induced exosomes which are released under pathological conditions have attracted increasing attention [8-10]. Vicencio *et al.* reported that plasma exosome quantity was increased under ischemic stress. These stress-induced exosomes could transfer Hsp70 to cardiomyocytes, thus activating the ERK pathway [9]. Zhang *et al.* reported the function of serum exosomes from patients with atherosclerosis and showed that they promoted endothelial cell migration by exosomal delivery of miR-150 to endothelial cells [11]. Whether the exosomes under myocardial ischemia conditions could play a regulatory role on endothelial cells is still not clear.

In this study, we investigated the role of coronary serum exosomes from the patients with myocardial ischemia (isc-Exo) and healthy controls (con-Exo), and evaluated their angiogenesis effects and miRNA profiles. We also revealed that pro-angiogenesis exosomes might be released from ischemic cardiomyocytes and were delivered to endothelial cells. The isc-Exo had lower levels of miR-939-5p compared to con-Exo which promoted endothelial angiogenesis through the iNOS-NO pathways.

Materials and Methods

Patients

Patients with chest pain and electrocardiogram evidences of suspected myocardial ischemia in the past three months who underwent diagnostic cardiac catheterization in Shanghai East Hospital were enrolled in this study. Exclusion criteria included: 1) diabetes (fasting glucose > 7.0 mM or postprandial glucose > 11.1 mM); 2) poorly controlled blood pressure; 3) hyperlipidemia (total cholesterol > 5.9 mM or total triglyceride > 2.26 mM); 4) evidence of infections; 5) other contraindications such as cancer, hepatic or nephritic diseases. After the angiography procedure, patients who had more than 70% stenosis were collected as the ischemic group. These patients were diagnosed as stable angina or acute coronary syndrome (ACS). Those with less than 50% stenosis or without stenosis were collected as the control group. These patients were eventually diagnosed as stable angina or myocardial bridge. All the enrolled patients had signed the informed consent form and the experiments were approved by the Shanghai East Hospital Ethics Committee.

Exosome isolation

Exosomes were isolated from the sera of the ischemic group and control group. 10 mL blood was drawn from the Johnson's Cordis 5F or 6F catheter into a sterile centrifuge tube from the aortic sinus. After that, all the blood samples were centrifuged at 2,400 g for 10 minutes at 4 °C to remove cells and debris, then the supernatants were centrifuged at 860 g for 10 minutes at 4 °C to further purify the serum. The serum exosomes were isolated using the ultracentrifugation method. Briefly, 1 mL serum was diluted in 10 mL PBS and filtered by a 0.22 μm filter. Then the samples were centrifuged at 150,000 ×g at 4 °C overnight. The supernatant was discarded and the exosome pellet was dissolved in 11 mL PBS. Then the samples were centrifuged at 150,000 ×g 4°C for 2 h [12]. The final exosome pellets were dissolved in 50 μL RIPA lysis buffer (Beyotime, P0013C) and quantified by the protein concentration. BCA Protein Assay kit (Thermo, 23225) was used to determine the exosome protein concentration as previously described. The pellets were also dissolved in 500 μL TRIzol reagent (Invitrogen, 15596026) for RNA evaluation and 250 μL PBS for exosome downstream analysis.

Electron microscopy

Transmission electron microscopy was conducted to identify the morphology of serum-derived exosomes as previously described [13]. After fixation by 1% glutaraldehyde for 2 h at room temperature, exosomes were loaded on carbon-coated electron microscopy grids and negatively labeled with phosphotungstic acid for 5 min. The microscopy images were captured by a JEOL JEM-1400 transmission electron microscope operating at 120 kV.

Western blot analysis

Western blot was used to identify the surface markers of exosomes: CD9 (Abcam, ab92726); CD63 (Abcam, ab134045); Flotillin (Abcam, ab41927) and protein levels of Alix (Abcam, ab186429); Tsg101 (Abcam, ab125011); Rab11a (Abcam, ab128913); iNOS

(Novusbio, NB300-605). Briefly, 5x loading buffer was mixed with protein lysis and heated at 95 °C for 5 min. Then, the samples were loaded on 12% SDS-PAGE polyacrylamide gels and run at 80V for 30 min before 120V for 1 h and then transferred to the polyvinylidene fluoride membrane at 300mA for 1 h. The membrane was incubated in 5% nonfat milk (CST, 9999s) and then exposed to the primary antibody: anti-CD9 (1:500); anti-CD63 (1:200); anti-flottilin (1:5000); anti-Alix (1:1000); anti-Tsg101 (1:1000); anti-Rab11a (1:5000); anti-iNOS (1:200) at 4°C overnight. After carefully washing with 1x Tris-buffered saline with tween, the membrane was incubated with secondary antibody (1:10000) at room temperature for 1 h. The protein band was detected and captured by LI-COR Odyssey Infrared Imaging.

Quantitative RT-PCR analysis

qPCR analysis was performed for gene expression. Briefly, RNA was extracted by TRIzol reagent (Invitrogen, 15596026) and reverse-transcript reaction was conducted using the PrimeScript RT reagent kit (TaKaRa, RR047A). The miRNA reverse transcription and qPCR primers were purchased from Guangzhou Ribobio Corporation. The iNOS primers were: CAGCGGGATGACTTTCCAA (forward) and AGGCAAGATTTGGACCTGCA (reverse). The β-actin primers were: AGGCATCCTCACCCTGAAGTA (forward) and CACACGCAGCTCATTGTAGA (reverse) as previously reported [14]. The qPCR was conducted using the SYBR Premix Ex Taq II kit (TaKaRa, RR820A) on an Applied Biosystems 7500 Real-Time PCR System. The relative expression level was calculated by the $2^{(-\Delta\Delta CT)}$.

Cell culture

Primary rat neonatal cardiomyocytes, mouse cardiac endothelial cells, HUVEC, and NIH3T3 cell lines were cultured as previously described. Briefly, primary cardiomyocytes were harvested by collagenase II digestion and confirmed by immunofluorescence staining with specific markers [15]. The mouse primary endothelial cells were harvested by collagenase I digestion and CD31 magnetic bead separation and cultured in EGM-2 media (Lonza, 3162). 4.5 g/L glucose DMEM (Gibco, 11965) containing 10% FBS was used to culture the primary cardiomyocytes and cell lines. The cells were incubated in an incubator at 37 °C, 5% CO_2. The hypoxia experiments were conducted using the Genbag (BioMerieux, 45534). The cells were incubated under hypoxia conditions for 24 h.

Interactions between HUVECs and exosomes

Exosome staining was conducted as previously described [16]. 0.25 μL Calcein AM (Invitrogen,

L3224) was used to label 100 μL exosomes dissolved in PBS at 37 °C for 20 min. Then 100 μL labeled exosomes were diluted in 400 μL DMEM and incubated with HUVECs for 6 h. The HUVECs were then labeled with Phalloidin (CST, 8953) (1:200) and DAPI (1:10000) at room temperature for 15 min. The cells were then captured using a Leica Confocal Laser Scanning Microscope and the images were 3D reconstructed using confocal Z-stack images [17].

Cell proliferation

Cell proliferation was assessed by the cell counting kit-8 (Dojindo, CK04-11), Cell-Light EdU kit (Ribobio, C10310-3) and also by manual cell counting. Briefly, 100 μL cell suspension containing 3000 cells was dispensed in a 96-well plate. The HUVECs were treated with different doses of isc-Exo (100 μg/mL or 200 μg/mL); con-Exo (100 μg/mL or 200 μg/mL) and PBS. After 24 h, 10 μL CCK-8 reagent was added to the medium and incubated for 3 h. The OD level was measured by the spectrophotometric microplate reader at 450 nm. For EdU analysis, the reagent was added to the 96-well plate and incubated for 2 h to label EdU. Then the cells were captured by the Leica Fluorescence Microscope.

Cell migration analysis

HUVEC migration was analyzed using 8.0 μm Transwell inserts (Corning, 3422) and the scratch wound assay. In detail, cells were resuspended in serum-free DMEM and 2×10^5 cells per well were seeded into the Transwell inserts to allow the cells to migrate through the 8.0 μm pore polycarbonate membrane to the underside with DMEM containing 10% FBS. The cells were then treated with isc-Exo or con-Exo or PBS and incubated for 8 h at 37 °C, 5% CO_2. At the time point, cells inside each insert were removed with cotton swabs and the migrated cells on the underside were stained with crystal violet solution for 10 min and counted in five microscopic random fields. The scratch wound assay was conducted by resuspending HUVEC in 6-well plates and starving for 12 h before experiments. The scratch wound was generated by a pipette tip. isc-Exo, con-Exo or PBS were used respectively. After 18 h, the wound area was observed and analyzed. The ratio of non-migrated area divided by the baseline area was used to calculate the migration effects.

Matrigel tube formation

In vitro tube formation analysis was evaluated on 50 μL Matrigel Matrix (BD, 356234) in a 96-well plate. 2×10^4 cells per well were dispensed onto the Matrigel. Then the cells were treated with isc-Exo, con-Exo and PBS. After incubating for 8 h, the tube formation was

analyzed by calculating the number of nodes and total tube length.

Evaluation of iNOS activity and NO levels

The iNOS activity of the cell supernatant was evaluated by the NOS Activity kit (Nanjing Jiancheng, A014) and supernatant NO levels were evaluated by the Griess Reagent kit (Invitrogen, G7921). Briefly, HUVECs were seeded in 6-well plates and the cells were then treated with mimic, inhibitor or scrambled miRNA for 72 h. Cell supernatants were thereafter obtained and centrifuged at 95 g for 5 min to remove debris. The supernatants were added to 96-well plates and the reagents of the NOS Activity kit or the Griess Reagent kit were added and incubated according to the protocols. The absorbance was measured at 530 nm and 548 nm, respectively, by a spectrophotometric microplate reader.

Animals

Wild type, male C57BL/6 mice aged 10-12 weeks and new born SD rats were purchased from Shanghai Sippr-BK Laboratory Animal Co. Ltd. The animals were fed under a specific pathogen free environment in the Shanghai East Hospital animal laboratory. All animal experiments were conducted under the rules approved by the Shanghai East Hospital Ethics Committee.

Mouse model of hind-limb ischemia and myocardial infarction

Unilateral hind-limb ischemia was conducted as previously described [18] by surgically excising and ligating the two sides of the left femoral artery from the proximal iliac-femoral artery to the distal branch of the femoral common artery. The right limb was left as control. One day after the surgery, the hind-limb was measured by Laser-Doppler Perfusion Imaging to ensure the effects of ligation. Meanwhile, isc-Exo and con-Exo were diluted with PBS to a final concentration of 1×10^3 µg/mL and the hind-limb ischemic mice were randomly treated with 200uL isc-Exo, con-Exo or PBS (n = 5 per group) by quadriceps muscle injection using a 1mL syringe. After the injection, Laser-Doppler Perfusion Imaging was used to monitor the blood flow recovery at 7, 14 and 21 days. The hind-limb blood flow perfusion was assessed by the ratio of ischemic limb divided by the control limb. The myocardial infarction model was conducted as previously described [19]. Briefly, the mice were anaesthetized and intubated. The heart was exposed by separating the ribs. The left anterior descending coronary artery was then ligated. The chest was then closed. The ischemic zones were collected 3 days after the myocardial infarction.

Microarray and data analysis

Total RNA was extracted from the isc-Exo and con-Exo groups by using the miRNeasy Mini Kit (Qiagen, 217004). The RNA was quantified by Thermo ND-2000 NanoDrop and Agilent 2100 Bioanalyzer. Six Agilent Human miRNA (8*60K, Design ID: 070156) microarrays were used in the experiment. The RNA labeling and array hybridization were conducted using the miRNA Complete Labeling and Hyb Kit (Agilent technologies, 5190-0456) according to the manufacturer's instructions. Slides were scanned by Agilent Microarray Scanner (Agilent technologies, G2 565CA) and Agilent Feature Extraction software v10.7 with default settings. Raw data were normalized by the Quantile algorithm in the R software [20].

After acquiring the raw data, the differently expressed miRNAs were calculated using the *t*-test. Those with ≥ 2-fold change and *P*-value < 0.05 were regarded as significantly different. Volcano plots and heat maps were generated by using Microsoft Excel 2010. The function analysis was conducted using the GO analysis (http://www.geneontology.org) to show the involved biological functions. The pathway analysis was conducted using the KEGG. The GO and KEGG results were ranked by enrichment factors, which were used to reveal the most associated functions and pathways.

Histological and immunofluorescence analysis

The ischemic muscles after 21 days were harvested, paraformaldehyde fixed and embedded in paraffin. The sections were stained by hematoxylin and eosin. For immunohistochemistry and immunofluorescence staining, the sections were incubated with primary antibody: CD31 (CST, 3528s) (1:100); α-SMA (Abcam, ab7817) (1:50) overnight, followed by secondary antibody.

Luciferase assay

A dual-luciferase reporter assay system and Sirius single tube luminometer were used to test luciferase activity. The 3'-UTR of the iNOS sequence containing the predicted miR-939-5p binding sites and its mutant were cloned into the plasmid vector and transfected into HEK293 cells. A Renilla luciferase vector was co-transfected in all transfections described to monitor transfection efficiency. All luciferase results were reported as relative light units: the average of the Photinus pyralis firefly activity observed divided by the average of the activity recorded from the Renilla luciferase vector.

Statistical analysis

All the experiments were repeated at least three times and all the data are shown as mean ± standard

errors of the mean. Unpaired *t*-test was used to analyze the differences between groups and a *P*-value < 0.05 was regarded as statistically significant.

Result

Characterization of serum exosomes

Twenty patients were enrolled in the study. The baseline characteristics of the enrolled patients are shown in Table 1. The two kinds of serum exosomes were purified by the ultracentrifugation method as previously reported [12]. Nanosight analysis showed that the particle size distribution of the two kinds of purified exosomes were between 30-100 nm (Figure 1A). Transmission electron microscopy was used to identify the morphology of purified exosomes which showed a round, cup-shaped morphology ~50 nm in diameter, indicating that the main contents of the microvesicles were exosomes (Figure 1B, C). Meanwhile, specific exosome markers (CD9, CD63, Flotillin) were expressed in both the two kinds of exosomes (Figure 1D). All together, these results confirmed that the main contents of the purified microvesicles were exosomes.

Serum-derived exosomes were internalized by endothelial cells

To verify if the serum exosomes could interact with endothelial cells, the purified exosomes were labeled with Calcein AM and co-incubated with endothelial cells for 6 h. The endothelial cells were then labeled with Phalloidin and DAPI and captured by confocal microscope. The 3D Z-stack reconstruction images showed that the green-labeled exosomes were internalized and mainly located in the cytoplasm of endothelial cells after co-incubation, indicating that serum exosomes could indeed interact with endothelial cells (Figure 1E).

Isc-Exo promoted endothelial cell proliferation, migration and tube formation

Previous studies indicated that exosomes could act as cargos to transport regulatory signals. In order to determine the effects of serum-derived exosomes on endothelial cells, HUVECs were co-incubated with both kinds of exosomes. In the proliferation analysis, isc-Exo better promoted endothelial cell proliferation compared to con-Exo after 24 h of treatment, as indicated by the Edu and CCK8 analyses (Figure 2A-C). Follow-up manual cell counting also confirmed the above results (Figure 2D). Meanwhile, the proliferative effect of exosomes on endothelial cells showed a dose-dependent response. In addition, vascular formation ability was assessed by Matrigel assay and it revealed that isc-Exo increased the number of nodes and total tube length compared to con-Exo, indicating its pro-angiogenesis ability (Figure 2E-G). Furthermore, transwell and scratch wound assay were used to determine the migration of endothelial cells after treatment by the two kinds of exosomes. It was shown that both isc-Exo and con-Exo could promote the migration of endothelial cells, while isc-Exo showed greater effects than con-Exo both by migrated area in the wound assay (Figure 2H, I) and migrated number of cells in the Transwell assay (Figure 2J, K). Overall, isc-Exo showed prior effects than con-Exo in angiogenesis-related processes including proliferation, migration and tube formation, indicating that exosomes derived from coronary serum of patients with myocardial ischemia might contain some different angiogenesis signals compared to exosomes from controls. Hence, coronary serum-derived exosomes were angiogenesis regulators while isc-Exo showed prior effects.

Isc-Exo promoted angiogenesis in mouse hind-limb ischemia

To further determine the *in vivo* angiogenesis effects of isc-Exo and con-Exo, a mouse hind-limb ischemia model was generated and the two kinds of exosomes were intramuscularly injected 1 day after the surgery. At 7 and 14 days post-surgery, the isc-Exo and con-Exo groups did not show an advantage in blood flow recovery compared to the PBS group. However, after 21 days post injection, the isc-Exo group showed a significantly 2-fold higher blood perfusion than the con-Exo group. Meanwhile, there was no significant difference in blood perfusion between the con-Exo group and the PBS group showing that isc-Exo promoted ischemic injury repair while con-Exo did not (Figure 3A, B). In addition, the ischemic limb skin appearance of the three groups at 21 days also showed a similar trend. There was no scar or ischemic appearance on the ischemia limb skin in the isc-Exo group after 21 days, while we could see scarring in the PBS group and swelling in the con-Exo group (Figure 3C). Further, muscle samples were harvested, sectioned and stained. The angiogenesis ability after the ischemia was determined by vascular marker CD31.The isc-Exo group showed a significantly higher capillary density compared to the con-Exo group both by immunohistochemistry (Figure 3E) and immunofluorescence (Figure 3F), indicating isc-Exo's potential role in microvascular construction. Overall, the *in vivo* mouse limb ischemia analysis revealed that, compared to the con-Exo group, the isc-Exo group significantly increased the capillary density, thus enhancing the post ischemic injury repair. Coronary serum-derived exosomes were positive regulators in post ischemia recovery while isc-Exo showed stronger healing ability.
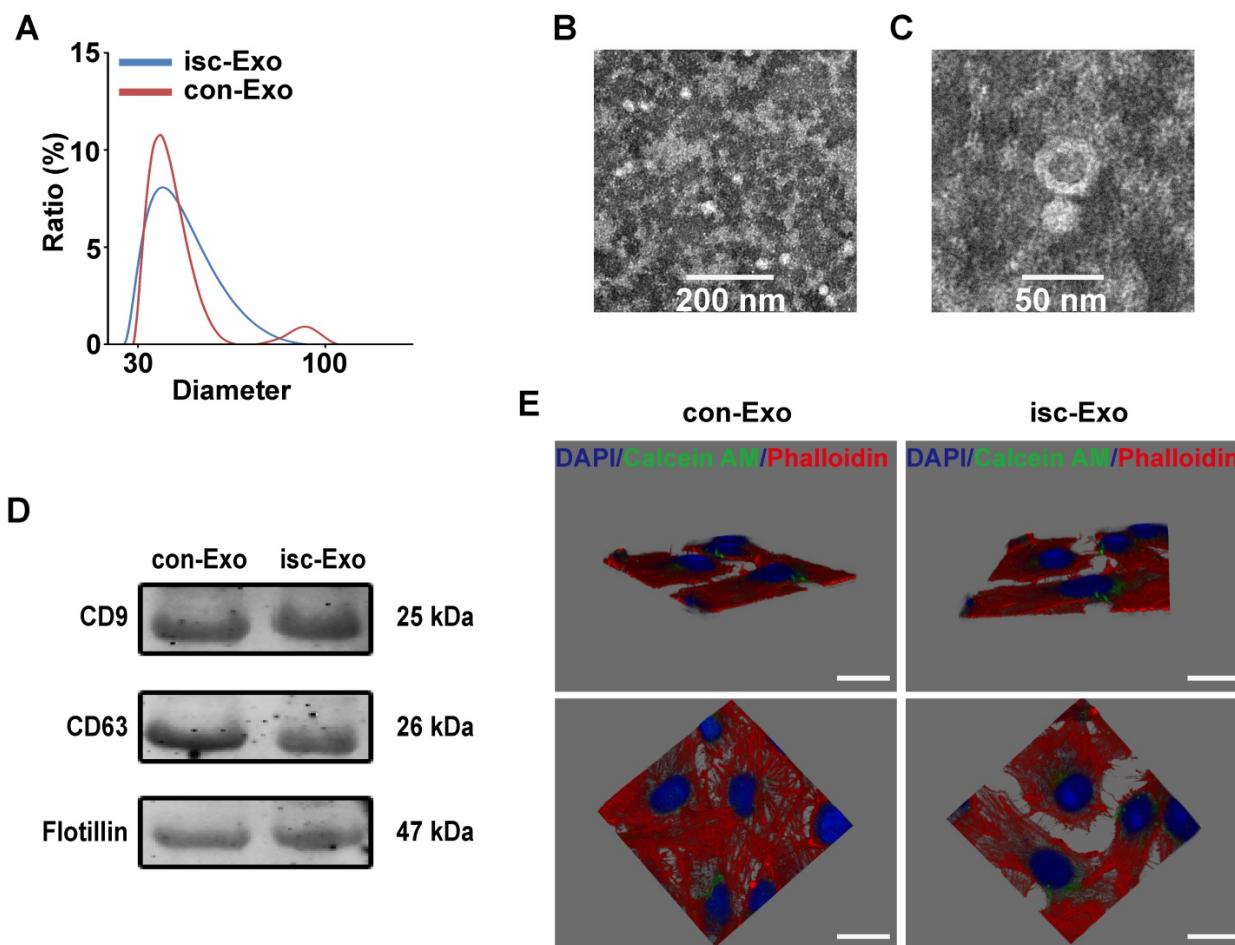
Figure 1. Characterization and internalization pathways of coronary serum exosomes. (A) The particle diameter distribution ratio measured by Nanosight analysis of isc-Exo (blue) and con-Exo (red), which indicated that most of the particles were between 30-100 nm. (B, C) The transmission electron microscopy appearance of exosomes. Bars indicate 200 nm and 50 nm, respectively. (D) The CD9, CD63 and Flotillin expression levels in both con-Exo and isc-Exo. (E) Representative horizontal and vertical images of a 3D Z-stack reconstruction showing labeled exosomes (green) were located in HUVEC cytoplasm (red). Bars indicate 10 μm.

Pro-angiogenic isc-Exo might be secreted by hypoxic cardiomyocytes

In order to investigate the source of the pro-angiogenic exosomes in coronary serum, exosome biogenesis-related marker proteins (Alix, Tsg101 and Rab11a) were evaluated in the main kinds of cardiac cells (cardiomyocytes, fibroblasts and endothelial cells). We first generated the mouse myocardial infarction model and evaluated the protein levels in the border zones of the ischemic myocardium. This revealed that Alix was strikingly up-regulated in the ischemic myocardium (Figure 4A). In addition, in primary cardiomyocytes treated with hypoxia, Alix and Rab11a were up-regulated (Figure 4B), while in hypoxic endothelial cells (Figure 4C) and fibroblasts (Figure 4D), the three proteins remained unchanged and even down-regulated. In conclusion, ischemic and hypoxic stress up-regulated the exosome biogenesis-related proteins in specific cell types, thus

initiating the biogenesis of exosomes. We assumed that the ischemic cardiomyocytes might be the source of functional exosomes in this situation.

Table 1. The baseline characteristics of enrolled patients.

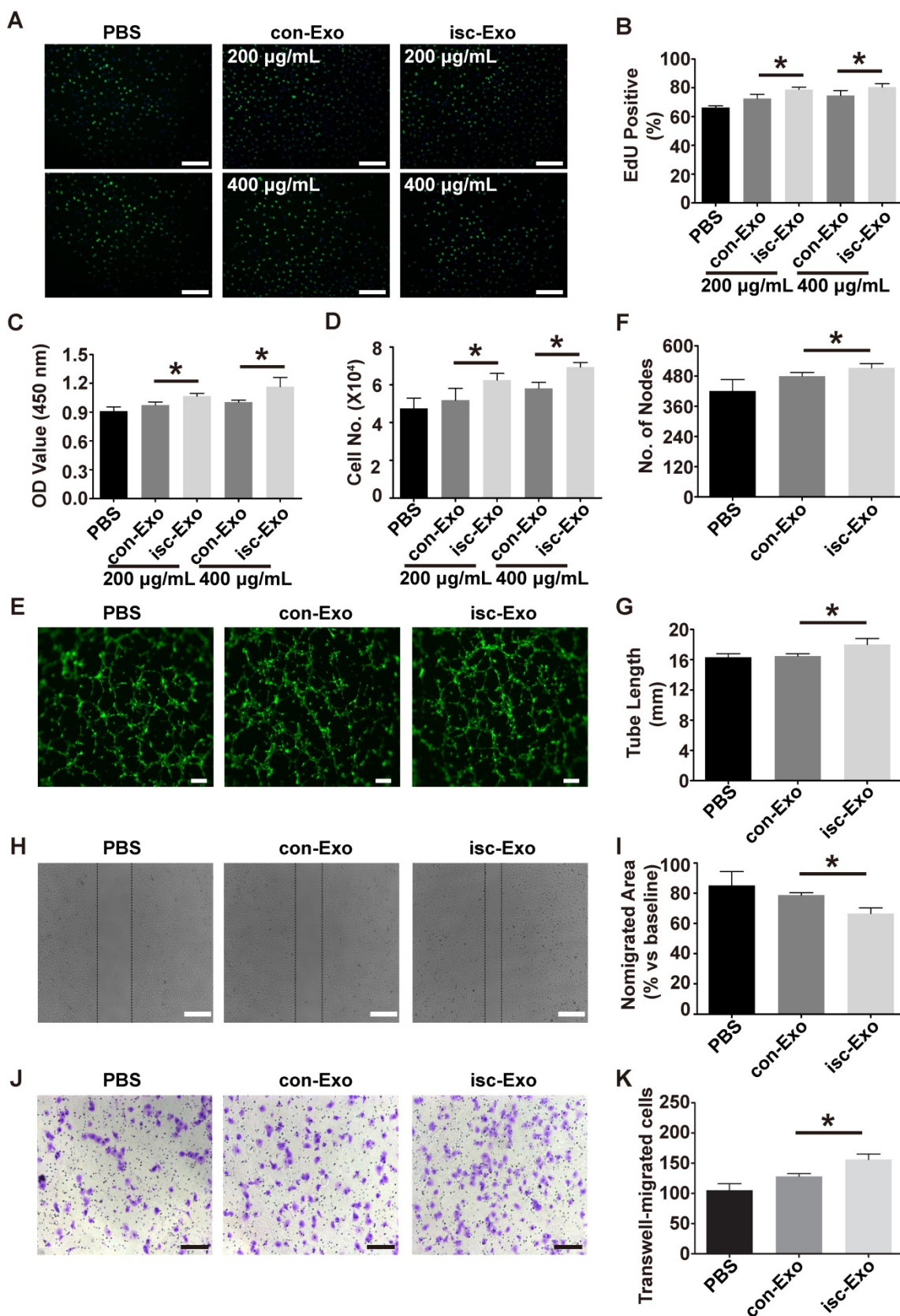| Characteristics	Ischemia (N = 10)	Control (N = 10)
Age (year)	69.6±8.2	61.7±7.1
Male (%)	80	60
Glucose (mM)	5.3±1.8	5.8±1.4
Cholesterol (mM)	3.6±0.8	3.6±1.0
Triglyceride (mM)	1.2±0.4	1.4±0.5
LDL (mM)	1.8±0.6	1.9±0.5
TnT positive (%)	30	0
Characteristics of lesion		
LAD (%)	60	50
LCX (%)	20	10
RCA (%)	20	20
Statins (%)	90	50
ACEI&ARB (%)	60	40
LV dysfunction (%)	10	0
PCI history (%)	90	20

Figure 2. Effects of isc-Exo and con-Exo on *in vitro* angiogenesis. (A, B) The isc-Exo group showed greater proliferative effects than con-Exo at both 200 μg/mL and 400 μg/mL doses in EdU-positive cells measured by CCK8 absorbance (C) and manual cell count (D). (E) The isc-Exo group showed better vascular formation ability than con-Exo in tube formation analysis measured by number of nodes (F) and tube length (G). isc-Exo promoted endothelial cell migration, as evaluated by scratch wound assay (H) and analyzed by the ratio of non-migrated area divided by the baseline wound area (I). (J) The Transwell assay also revealed the same trend as the wound assay and was analyzed by the number of migrated cells (K). Bars indicate 200 μm in all pictures. * indicates P < 0.05.
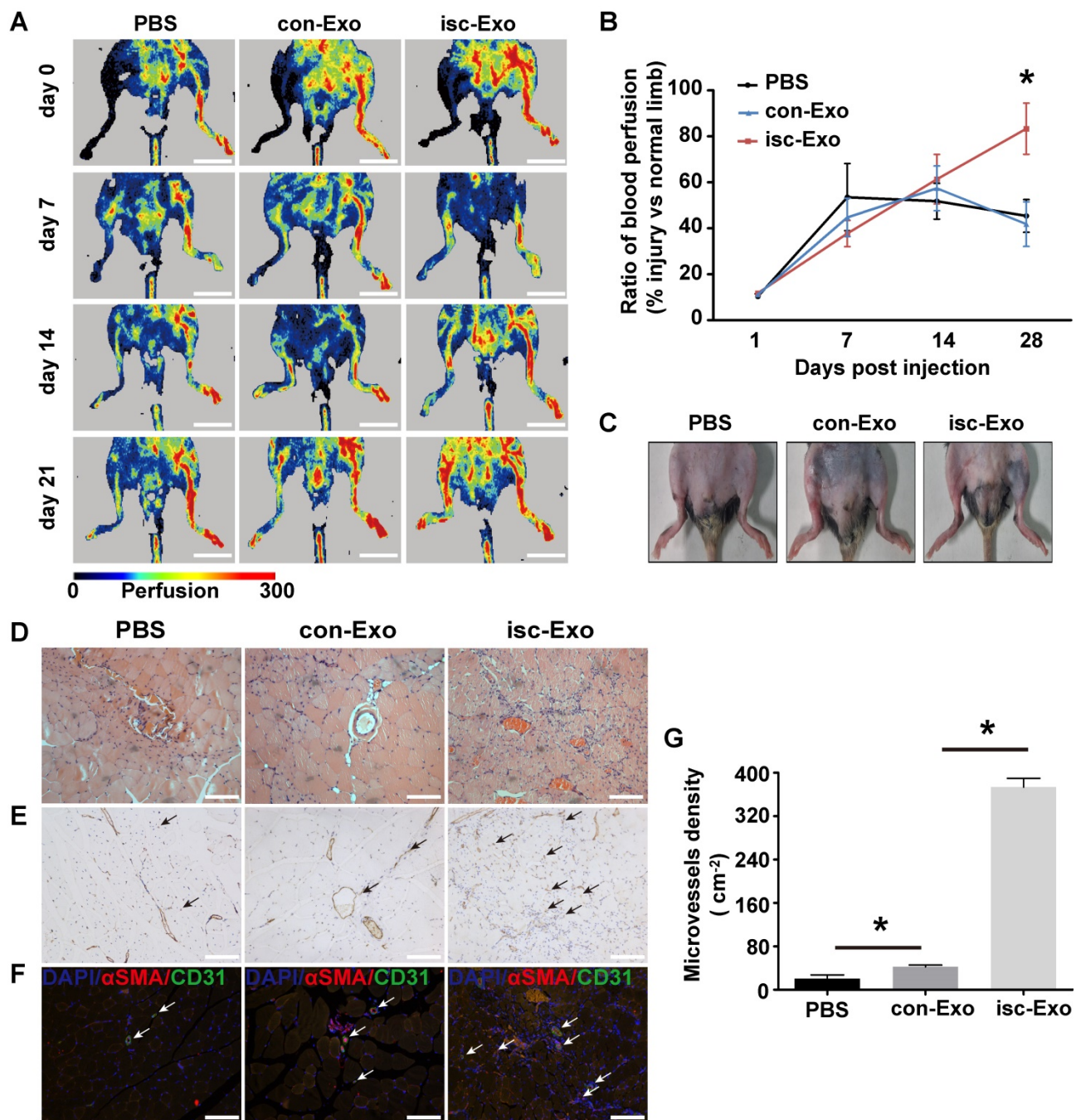
Figure 3. Healing effects of isc-Exo and con-Exo on mouse ischemic injury after hind-limb ischemia. (A) Blood flow recovery evaluated by Laser-Doppler perfusion imaging 0, 7, 14, 21 days after surgery. The left side was the ischemia limb and the right side was the normal control limb. Bars indicate 1 cm. (B) The healing effect of blood perfusion recovery was analyzed by the perfusion ratio of the ischemia side divided by that of the normal control side. The isc-Exo group showed better blood perfusion recovery effects compared to the con-Exo group 21 days after surgery. (C) The ischemic limb skin appearance 21 days after surgery. The PBS group showed scarring on the left ischemia limb and the con-Exo group showed swelling in the whole ischemia limb. Meanwhile, the isc-Exo group showed a better recovery. Muscle sections stained by hematoxylin and eosin (D), CD31 immunohistochemistry (E) and CD31 and α-SMA immunofluorescence (F). The arrows indicate the microvessels in the muscle and the bars indicate 100 μm in the pictures. red: α-SMA, green: CD31, blue: DAPI. (G) The capillary density in the ischemia muscles was analyzed by the number of microvessels per cm². The isc-Exo group showed higher capillary density than the con-Exo group. * indicates P < 0.05.

miR-939-5p was down-regulated in isc-Exo

Both the *in vitro* and *in vivo* analyses revealed that isc-Exo enhanced angiogenesis compared to con-Exo. To investigate the underlying angiogenic roles in exosomes, we further explored the miRNA profile of isc-Exo and con-Exo as previous studies indicated that miRNAs are one of the main functional contents in exosomes. In order to identify the miRNA profile of isc-Exo and con-Exo, we chose three ACS patients and three control patients and collected their serum exosome samples to conduct a microarray

analysis. In the end, five miRNAs (miR-939-5p, miR-1246, miR-3679-5p, miR-4787-3p and miR-6085) were found to be down-regulated and one (miR-4307) was found to be up-regulated in isc-Exo compared to con-Exo. The differently expressed miRNAs were shown as a volcano plot and a heat map (Figure 5A, B). Follow-up qPCR verification showed a similar trend as the microarray results (Figure 5E). Bioinformatics analyses including GO and KEGG analyses were then conducted to reveal the most related processes and pathways. The most enriched biological processes were cardiac conduction communication, TGF-β regulation, glucose transcription and heart morphology apoptosis, indicating that the exosomes were involved in various biological processes including cardiac cell communication and immune regulation (Figure S1A). To further investigate the endothelial- and cardiomyocyte-related processes, we screened the related GO terms and found that the differently expressed miRNAs were mainly associated with endothelial cell differentiation, fate commitment, migration, proliferation and cell chemotaxis which revealed the potential role of these miRNAs in endothelial differentiation and angiogenesis-related processes (Figure 5C). Meanwhile, the differently expressed miRNAs were mainly related to cardiomyocyte conduction, relaxation, membrane potential, differentiation and tissue growth (Figure 5D). In order to find out the functional miRNAs involved in the endothelial cell regulation, gain-of-function analysis was conducted by transfecting miRNA mimics into HUVEC. We chose miR-939-5p, miR-1246, miR-4787-3p and their mimics were transfected for 24 h. The cell proliferation was then evaluated and showed that endothelial cell proliferation was inhibited by miR-939-5p and miR-4787-3p but not by miR-1246, compared to the control mimic (Figure 5F). As miR-939-5p has been reported to be involved in angiogenesis, we chose miR-939-5p for further down-stream analysis.
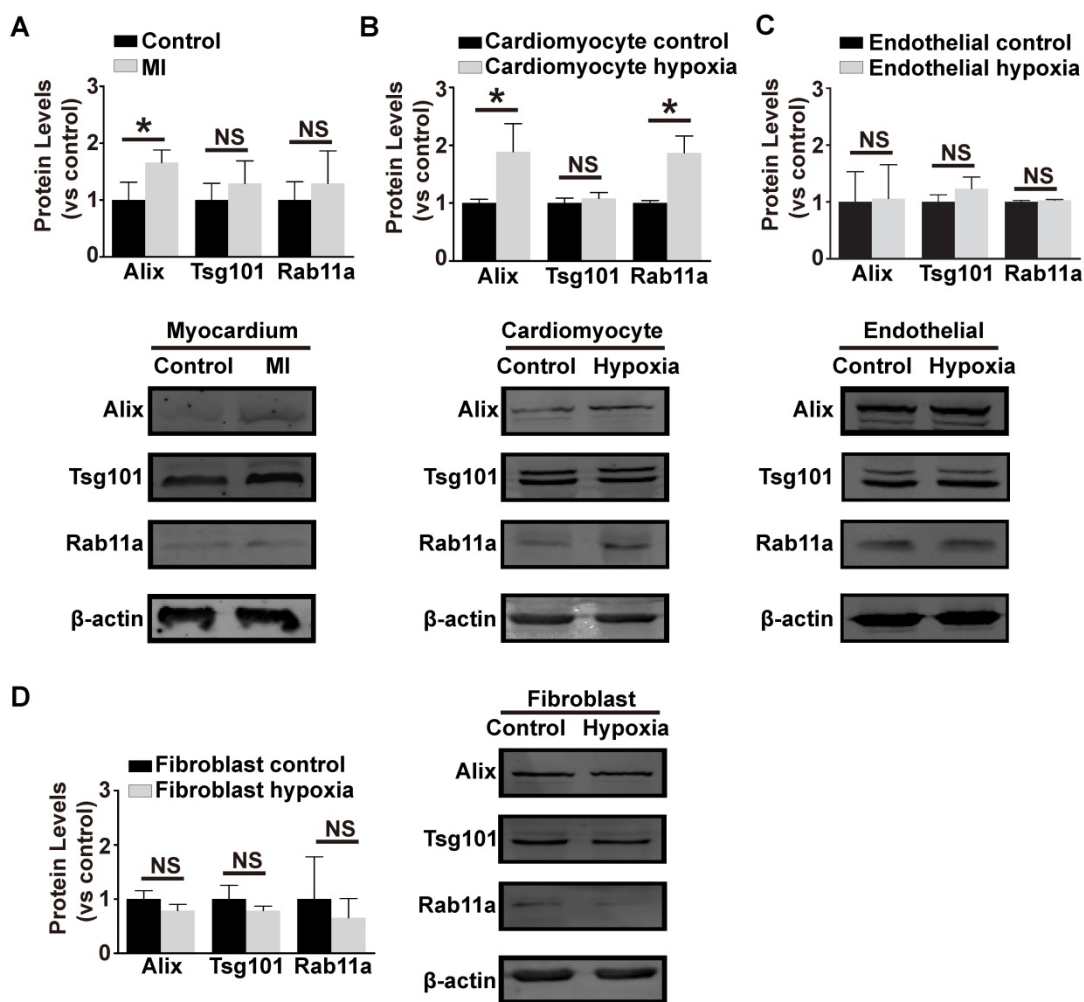

Figure 4. Exosome biogenesis related proteins under hypoxia stress. The expression of exosome biogenesis-related proteins Alix, Tsg101 and Rab11a in ischemic myocardium (A) primary cardiomyocytes (B) primary endothelial cells (C) and fibroblasts (D). Alix showed a higher expression in the ischemic myocardium and hypoxic cardiomyocytes. Rab11a was also higher in hypoxic cardiomyocytes. However, the hypoxic endothelial cells and fibroblasts did not show an increase in any of Alix, Tsg101 or Rab11a. * indicates P < 0.05 and NS indicates P > 0.05. The protein levels are shown as the experiment group divided by the control group.
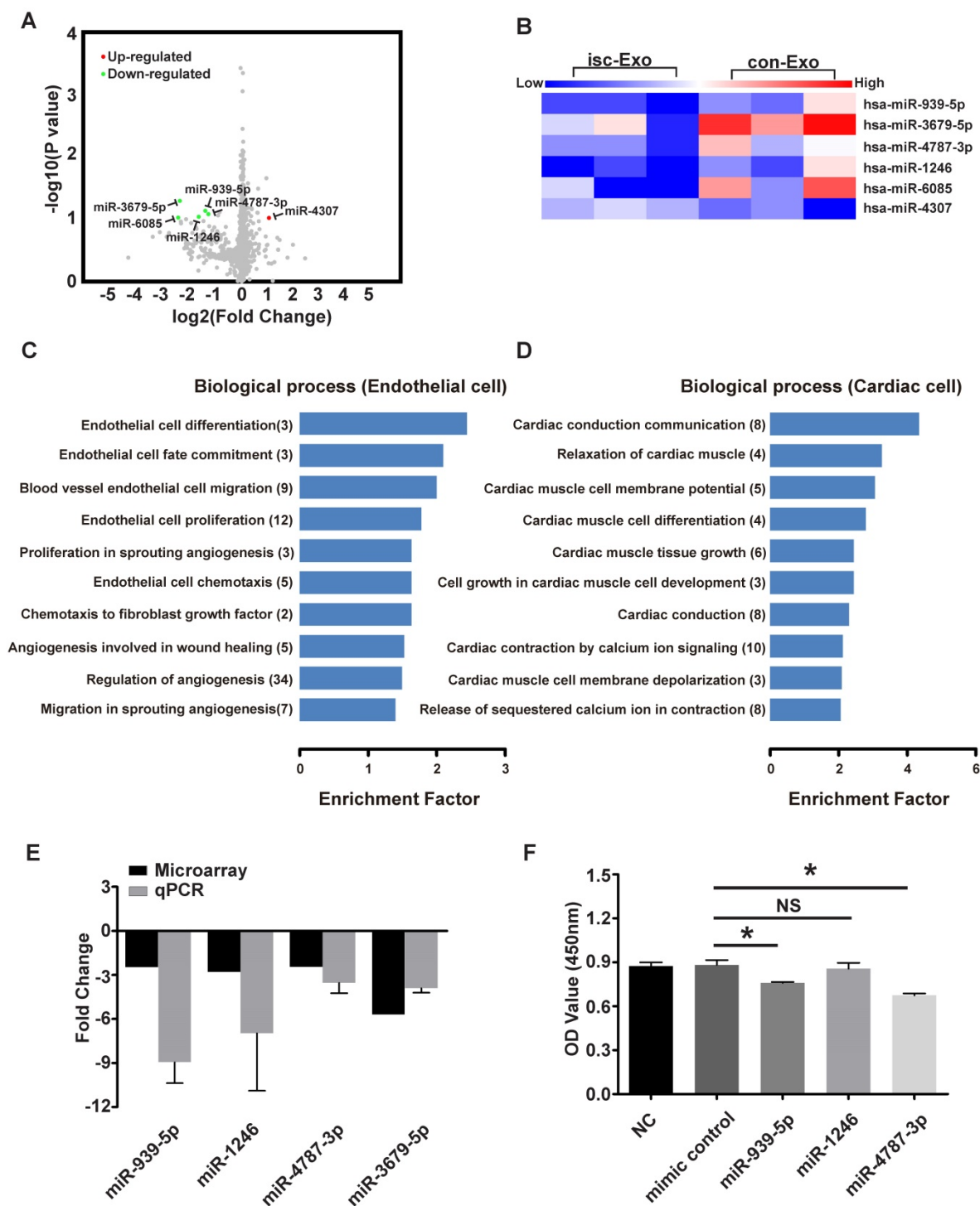
Figure 5. The microarray analysis of isc-Exo and con-Exo. (A) volcano plot and heat map (B) of isc-Exo and con-Exo (the red dots indicate up-regulated miRNAs and the green dots indicate the down-regulated miRNAs). For the regulated miRNAs, the GO analysis of biological processes involved in endothelial (C) and cardiomyocytes (D). The columns indicate the related GO terms depending on the enrichment factor and the numbers in the parentheses indicate the number of genes. (E) qPCR verification of the regulated miRNAs and the results are shown as fold changes. (F) Overexpression analysis of selected miRNAs (miR-939-5p, miR-1246, miR-4787-3p) for their proliferative effect on endothelial cells. miR-939-5p and miR-4787-3p repressed endothelial cell proliferation. * indicates P < 0.05 and NS indicates P > 0.05).

miR-939-5p attenuated endothelial cell proliferation and tube formation

To test whether miR-939-5p could regulate angiogenesis, the effect of miR-939-5p on endothelial cell proliferation and tube formation was evaluated. The miR-939-5p mimic and inhibitor were transfected into HUVEC for gain- and loss-of function analyses. From proliferation assay, miR-939-5p overexpression significantly attenuated endothelial cell proliferation,

as evaluated by CCK8, while miR-939-5p inhibitor could promote cell proliferation compared to the control side (Figure 6A). Tube formation was then evaluated on a Matrigel assay. The miR-939-5p mimic could significantly impair the vascular formation ability when evaluating the number of nodes and total tube length. In contrast, miR-939-5p inhibitor enhanced vascular formation capability compared to the inhibitor control, indicating its pro-angiogenesis effects (Figure 6B-D). Taken together, these data showed that miR-939-5p could strongly attenuate the angiogenesis ability by down-regulating angiogenesis-related activities including proliferation and tube formation. miR-939-5p could be an angiogenesis suppressor and inhibition of miR-939-5p promoted angiogenesis.

miR-939-5p targeted iNOS and regulated NO production

Previous studies have shown that miR-939-5p could regulate endothelial function by targeting VE-cadherin [21] and γ-catenin [22]. Guo *et al.* previously revealed that miR-939-5p down-regulated iNOS in cultured hepatocytes [14]. Combining bioinformatics analysis and previous results, we chose iNOS as a candidate target in endothelial cells. To verify if iNOS was the direct target of miR-939-5p, luciferase assay was conducted. The 3′-UTR of NOS2 (iNOS) sequence containing the predicted miR-939-5p binding sites was cloned into the plasmid vector and the plasmid vector was transfected into HEK293 cells. miR-939-5p mimic or control were then transfected into HEK293 cells and the luciferase activity was tested. miR-939-5p mimic strikingly down-regulated the luciferase activity in the iNOS 3′UTR WT group but did not suppress luciferase activity in the iNOS 3′UTR Mut group (Figure 6E). The above results confirmed that iNOS was the direct target of miR-939-5p. To further investigate whether miR-939-5p could down-regulate iNOS in endothelial cells, the mimic and inhibitor of miR-939-5p were transfected into HUVEC and the mRNA and protein levels of iNOS were evaluated. After 72 h of transfection, the mRNA level of iNOS was knocked down by miR-939-5p and the inhibitor of miR-939-5p restored iNOS levels (Figure 6F). The western blot analysis also revealed that miR-939-5p overexpression could down-regulate iNOS protein levels in endothelial cells and miR-939-5p inhibitor up-regulated iNOS expression (Figure 6G, H). Furthermore, we also tested if miR-939-5p could influence the activity of iNOS in endothelial cells. The activity of iNOS was evaluated after transfection: the miR-939-5p mimic could down-regulate iNOS activity, while miR-939-5p knock-down improved

iNOS activity though there was no statistical difference (Figure 6I). NO levels were finally evaluated, which indicated that miR-939-5p overexpression could impair NO production, while miR-939-5p inhibitor enhanced NO production (Figure 6J). In order to test if eNOS, another important regulator of endothelial NO production, takes part in the regulatory pathways, we used nitroglycerin to induce the eNOS expression in endothelial cells. Previous studies indicated that nitroglycerin mainly induces NO production through the eNOS pathway [23]. In our study, nitroglycerin significantly increased NO levels; however, none of the miR-939-5p mimic or inhibitor could influence eNOS pathways (Figure S1E, F). In conclusion, miR-939-5p could target iNOS and down-regulate its mRNA and protein levels in endothelial cells. In addition, miR-939-5p attenuated the activity of iNOS thus repressing NO production.

Isc-Exo with lower miR-939-5p unlocked the iNOS signaling pathway in endothelial cells

To test if the miR-939-5p-iNOS pathway is truly involved in exosome regulation, we thus investigated the miR-939-5p and iNOS levels in isc-Exo- and con-Exo-treated endothelial cells. After treatment with exosomes for 72 h, the cellular miR-939 level was 3-fold higher in the con-Exo-treated endothelial cells (Figure 7A). The mRNA and protein levels of iNOS were both induced in the isc-Exo-treated group (Figure 7B-D), demonstrating an active iNOS pathway in endothelial cells. These results indicated that the lower miR-939-5p in isc-Exo could largely free the iNOS signaling pathway and thus achieve its angiogenic effect.

Discussion

Exosomes, which carry functional messages, play an essential role in cell-cell communication under both physiological and pathophysiological conditions [2, 24]. However, most of the studies have only investigated the exosomes derived from cultured cells or mice, knowledge about human sample-derived exosomes are still limited. In our current study, the exosomes were purified from human coronary blood which was drawn from a catheter positioned in the aortic sinus. Zhang *et al.* revealed that mouse cardiomyocytes could release cell-specific exosomes to the bloodstream under ischemic conditions [25]. We thus designed the study to draw blood from the places neighboring the ischemic myocardium, which might also release tissue- and cell-specific exosomes.
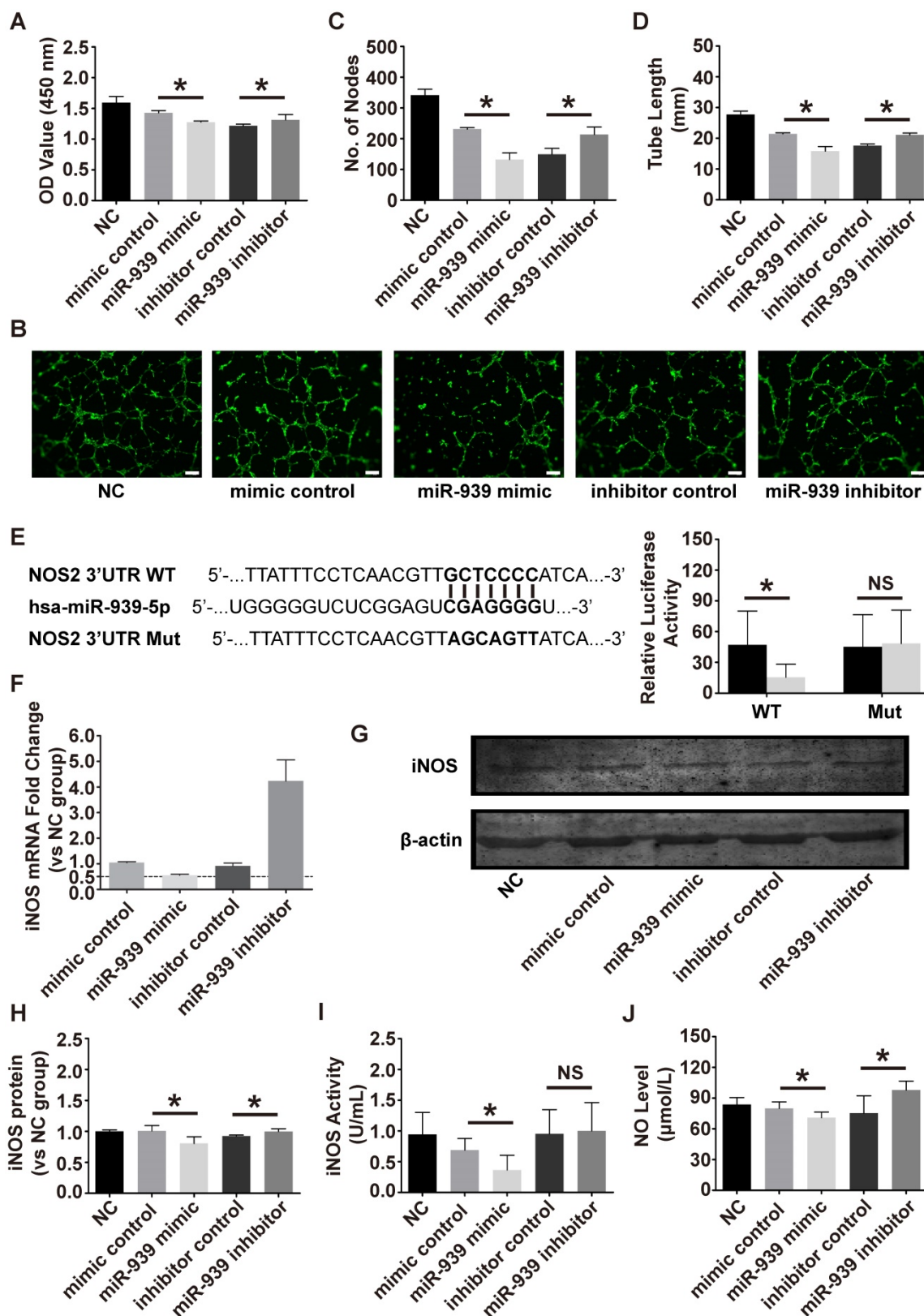
Figure 6. The effect of miR-939-5p on angiogenesis and down-stream targets. The effect of the miR-939-5p mimic or inhibitor on endothelial cell proliferation (A) and tube formation (B-D). The bar indicated 200 μm. miR-939-5p mimic strikingly repressed endothelial cell proliferation and tube formation and miR-939-5p inhibitor reserved the trend. (E) Plasmid vectors of human NOS2 (iNOS) 3'-UTR or its mutation were transfected into HEK293 cells followed by miR-939-5p mimic or control transfection. Dual luciferase activity assay showed that miR-939-5p mimic targeted iNOS 3'-UTR but not its mutation. The effect of miR-939-5p mimic or inhibitor on iNOS mRNA (F) and protein expression (G, H). miR-939-5p mimic significantly repressed iNOS mRNA and protein, while miR-939-5p inhibitor removed the suppression effects. The miR-939-5p mimic impaired iNOS activity (I) and the NO levels (J), while miR-939-5p inhibitor reserved the trend. * indicates P < 0.05 and NS indicates P > 0.05. The mRNA and protein expressions are shown as fold change vs. NC group.
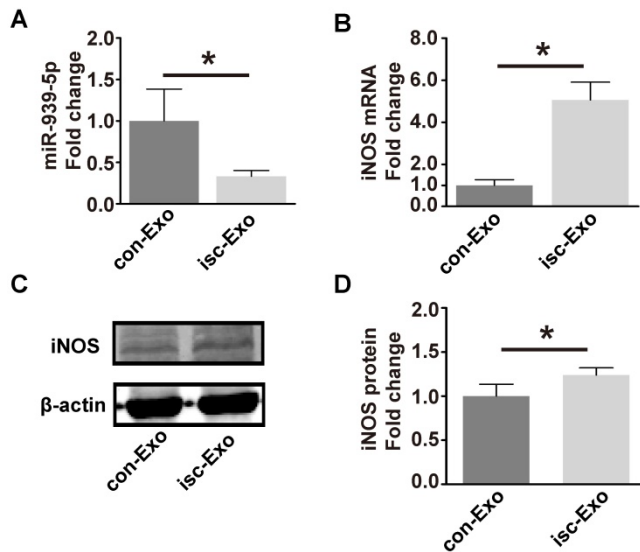
Figure 7. miR-939 and iNOS levels after isc-Exo and con-Exo treatment. (A) After treatment by isc-Exo and con-Exo, the miR-939 expression of con-Exo-treated cells was 3-fold higher than that of isc-Exo-treated cells. (B) Meanwhile, the iNOS mRNA level was 5-fold higher in the isc-Exo group. (C, D) The iNOS protein level in the isc-Exo-treated cells was also higher than that of con-Exo-treated cells. * indicates P < 0.05.

In this study, we found that both kinds of exosomes could be internalized by endothelial cells and isc-Exo accelerated endothelial cell proliferation, tube formation and migration. Meanwhile, isc-Exo showed a much better capability for post ischemic injury repair and angiogenesis than con-Exo in limb ischemia. To figure out the functional contents in exosomes, we conducted a microarray analysis to investigate the different miRNA profile in these two kinds of exosomes. As a result, miR-939-5p, miR-1246, miR-3679-5p, miR-4787-3p and miR-6085 were down-regulated, while miR-4307 was found to be up-regulated in the isc-Exo group compared to the con-Exo group. Further GO analysis revealed that the miRNAs were associated with endothelial cell differentiation, fate commitment, migration and proliferation. Then, miR-939-5p, miR-1246 and miR-4787-3p were evaluated by gain-of-function analysis in endothelial cells. Finally, miR-939-5p and miR-4787-3p showed significant suppression on cell proliferation. miR-939-5p has been reported to be involved in various biological processes [21, 22]. For example, Modica *et al.* revealed that miR-939-5p could impair the endothelial monolayer barrier thus promoting breast cancer metastasis [21]. In another study, miR-939-5p was reported to suppress endothelial cell angiogenesis by targeting γ-catenin [22]. Although these studies suggest the anti-angiogenic effects of miR-939-5p, the source and delivery route of miR-939-5p in ischemic disease remain unknown. Most importantly, the biological significance of miR-939-5p variation between ischemia and non-ischemia patients has not been evaluated.

Currently, we found that the serum exosomal miR-939-5p was lower in the myocardial ischemia compared to normal conditions. By manipulating miR-939-5p levels, the coronary serum-derived exosome acts as a messenger to regulate endothelial cell function and thus unlocks endogenous angiogenesis after myocardial ischemia. Previous studies reported that cardiomyocytes could release cell-specific exosomes to the bloodstream under ischemic conditions [25]. To explore the possible source of these angiogenic exosomes, both ischemic myocardium and hypoxic cardiomyocytes were studied. As a result, the exosome biogenesis-related marker proteins were activated in ischemic myocardium and hypoxic cardiomyocytes but not in endothelial cells or fibroblasts. These findings suggest that exosome biogenesis in cardiomyocytes is more sensitive to ischemic stress. Based on our findings and previous reports, we speculate that cardiomyocytes might be the source of angiogenic serum exosomes under ischemic conditions. By gain- and loss-of-function analyses, we found that miR-939-5p could repress angiogenesis by down-regulating endothelial cell proliferation and tube formation. Although the post-transcription inhibition of miR-939-5p on iNOS has been previously reported in cultured hepatocytes [14], we demonstrated that miR-939-5p directly targeted the 3'UTR of iNOS in endothelial cells and found that miR-939-5p acted as a repressor of both expression and activity of iNOS.

NO is widely involved in many physiological and pathological processes [26]. It is produced from L-arginine by NOS catalyst. In cardiovascular diseases, NO has been shown to exert many cardioprotective roles [27]. Previous studies indicated that NO is involved in smooth muscle cell [28], endothelial cell [29] and blood cell [30] regulation. In endothelial cells alone, NO was shown to enhance endothelial cell proliferation and migration and attenuated apoptosis [27, 31]. As many studies have demonstrated that NO is an essential mediator in VEGF-induced endothelial angiogenesis [32, 33], the lower level of miR-939-5p in endothelial cells after isc-Exo treatment may strengthen VEGF signal transduction, thus increasing angiogenic response.

Complicated origins and varying purification methods largely plague the study of circulating extracellular vesicles in cardiovascular diseases. Mallat *et al.* and Mizrachi *et al.* who have made some early researches in this area, found that in ACS patients, endothelial cell-derived microparticles were increased [34, 35]. Boulanger *et al.* further revealed

that microparticles derived from ACS patients would influence the eNOS pathway which in the end impaired NO capability [36]. These early studies used "microparticles" to describe the purified extracellular vesicles as they were shed mainly from various kinds of cells including platelets, leukocytes or endothelial cells which did not rigorously distinguish apoptotic bodies, microvesicles and exosomes [3]. However, these early studies clearly suggested the potential regulatory function of circulating extracellular vesicles. Recent studies have begun to focus on "exosomes" which are more specific than "microparticles" due to the promoted ultracentrifugation isolation methods [13]. With the rapid development of "-omics" technology, recent studies have also revealed that the protein profile of circulating exosomes after myocardial infarction is strikingly changed which provided potential biomarkers and novel targets for post-infarct regulation [37]. There was an interesting study [22] that investigated the circulating miRNAs in ischemic patients with sufficient or poor coronary collateral circulation. They found that circulating miR-939-5p is significantly down-regulated in the serum of sufficient coronary collateral circulation patients. The circulating miRNA, unlike the target-delivered exosomal miRNA, acts as a rover in circulation, which means it may react with any cell type the blood stream reaches. Since we found an exosome-mediated delivery of miR-939-5p to endothelial cells, it could better explain the fact that patients with lower levels of miR-939-5p patients have more sufficient collateral circulation.

There remain some limitations that we should acknowledge. First of all, the clinical sample size enrolled in this study was relatively small, which might neglect other functional miRNAs in patients with myocardial ischemia. Secondly, due to the complicated exosomal contents, the miR-939-iNOS-NO pathway might only be one of multiple pathways that regulate angiogenesis. The residual proteins in the purified exosomes might also play a role in exosome regulation.

In summary, the present study suggests that hypoxic cardiomyocytes may release functional exosomes (isc-Exo) into coronary artery serum, and isc-Exo acts as an angiogenic signal as its lower miR-939-5p level promotes NO production in endothelial cells. Our findings advance the current knowledge of endogenous angiogenesis with the novel route of exosomal miRNA in myocardial ischemia.

Abbreviations

ACEI: angiotensin-converting enzyme inhibitor; ACS: acute coronary syndrome; ARB: angiotensin receptor blocker; CCK-8: cell counting kit-8; con-Exo: control exosomes; DMEM: Dulbecco's Modified Eagle's medium; FBS: fetal bovine serum; GO: Gene Ontology; HUVEC: human umbilical vein endothelial cell; iNOS: inducible nitric oxide synthase; isc-Exo: ischemic exosomes; KEGG: Kyoto Encyclopedia of Genes and Genomes; LAD: left ascending artery; LCX: left circumflex artery; LDL-C: low density lipoprotein; MI: myocardial infarction; NO: nitric oxide; NOS2: nitric oxide synthase 2; PCI: percutaneous coronary intervention; RCA: right coronary artery.

Acknowledgements

Author Contributions

HL, HZ, and JG developed the idea and designed the whole study. HL, YL and LG performed experiments and analyzed the data. TZ and ZH provided kindly support in cell culture and sample collection. HL, HZ and JG wrote the manuscript. All the authors have reviewed and approved its final version.

Supplementary Material

Supplementary figure S1.
http://www.thno.org/v08p2079s1.pdf

Competing Interests

The authors have declared that no competing interest exists.

References

[1]. Benjamin EJ, Blaha MJ and Chiuve SE, et al. Heart Disease and Stroke Statistics-2017 Update: A Report from the American Heart Association. Circulation. 2017; 135: e146-e603.
[2]. Sluijter JP, Verhage V and Deddens JC, et al. Microvesicles and exosomes for intracardiac communication. Cardiovasc Res. 2014; 102: 302-11.
[3]. Andaloussi EL, Mager I and Breakefield XO, et al. Extracellular vesicles: biology and emerging therapeutic opportunities. Nat Rev Drug Discov. 2013; 12: 347-57.
[4]. Wang X, Huang W and Liu G, et al. Cardiomyocytes mediate anti-angiogenesis in type 2 diabetic rats through the exosomal transfer of miR-320 into endothelial cells. J Mol Cell Cardiol. 2014; 74: 139-50.
[5]. Wang X, Gu H and Huang W, et al. Hsp20-Mediated Activation of Exosome Biogenesis in Cardiomyocytes Improves Cardiac Function and Angiogenesis in Diabetic Mice. Diabetes. 2016; 65: 3111-28.
[6]. Zhang Z, Yang J and Yan W, et al. Pretreatment of Cardiac Stem Cells With Exosomes Derived From Mesenchymal Stem Cells Enhances Myocardial Repair. J Am Heart Assoc. 2016; 5: e002856.
[7]. Vrijsen KR, Sluijter JP and Schuchardt MW, et al. Cardiomyocyte progenitor cell-derived exosomes stimulate migration of endothelial cells. J Cell Mol Med. 2010; 14: 1064-70.
[8]. Porto I, Biasucci LM and De Maria GL, et al. Intracoronary microparticles and microvascular obstruction in patients with ST elevation myocardial infarction undergoing primary percutaneous intervention. Eur Heart J. 2012; 33: 2928-38.
[9]. Vicencio JM, Yellon DM and Sivaraman V, et al. Plasma exosomes protect the myocardium from ischemia-reperfusion injury. J Am Coll Cardiol. 2015; 65: 1525-36.
[10]. Hulsmans M and Holvoet P. MicroRNA-containing microvesicles regulating inflammation in association with atherosclerotic disease. Cardiovasc Res. 2013; 100: 7-18.

[11]. Zhang Y, Liu D and Chen X, et al. Secreted monocytic miR-150 enhances targeted endothelial cell migration. Mol Cell. 2010; 39: 133-44.

[12]. Melo SA, Luecke LB and Kahlert C, et al. Glypican-1 identifies cancer exosomes and detects early pancreatic cancer. Nature. 2015; 523: 177-82.

[13]. Thery C, Amigorena S and Raposo G, et al. Isolation and characterization of exosomes from cell culture supernatants and biological fluids. Curr Protoc Cell Biol. 2006; Chapter 3: Unit 3.22.

[14]. Guo Z, Shao L and Zheng L, et al. miRNA-939 regulates human inducible nitric oxide synthase posttranscriptional gene expression in human hepatocytes. Proc Natl Acad Sci USA. 2012; 109: 5826-31.

[15]. Deng S, Zhao Q and Zhen L, et al. Neonatal Heart-Enriched miR-708 Promotes Proliferation and Stress Resistance of Cardiomyocytes in Rodents. Theranostics. 2017; 7: 1953-1965.

[16]. Gray WD, Mitchell AJ and Searles CD. An accurate, precise method for general labeling of extracellular vesicles. MethodsX. 2015; 2: 360-7.

[17]. Lai CP, Kim EY, Badr CE, et al. Visualization and tracking of tumour extracellular vesicle delivery and RNA translation using multiplexed reporters. Nat Commun. 2015; 6: 7029.

[18]. Stabile E, Burnett MS and Watkins C, et al. Impaired arteriogenic response to acute hindlimb ischemia in CD4-knockout mice. Circulation. 2003; 108: 205-10.

[19]. Thal MA, Krishnamurthy P and Mackie AR, et al. Enhanced angiogenic and cardiomyocyte differentiation capacity of epigenetically reprogrammed mouse and human endothelial progenitor cells augments their efficacy for ischemic myocardial repair. Circ Res. 2012; 111: 180-90.

[20]. Lopez-Romero P. Pre-processing and differential expression analysis of Agilent microRNA arrays using the AgiMicroRna Bioconductor library. BMC Genomics. 2011; 12: 64.

[21]. Di Modica M, Regondi V and Sandri M, et al. Breast cancer-secreted miR-939-5p downregulates VE-cadherin and destroys the barrier function of endothelial monolayers. Cancer Lett. 2017; 384: 94-100.

[22]. Hou S, Fang M and Zhu Q, et al. MicroRNA-939 governs vascular integrity and angiogenesis through targeting gamma-catenin in endothelial cells. Biochem Biophys Res Commun. 2017; 484: 27-33.

[23]. Mao M, Sudhahar V and Ansenberger-Fricano K, et al. Nitroglycerin drives endothelial nitric oxide synthase activation via the phosphatidylinositol 3-kinase/protein kinase B pathway. Free Radic Biol Med. 2012; 52: 427-35.

[24]. Sahoo S and Losordo DW. Exosomes and cardiac repair after myocardial infarction. Circ Res. 2014; 114: 333-44.

[25]. Zhang X, Wang X and Zhu H, et al. Hsp20 functions as a novel cardiokine in promoting angiogenesis via activation of VEGFR2. PLoS One. 2012; 7: e32765.

[26]. Forstermann U and Sessa WC. Nitric oxide synthases: regulation and function. Eur Heart J. 2012; 33: 829-37.

[27]. Lei J, Vodovotz Y and Tzeng E, et al. Nitric oxide, a protective molecule in the cardiovascular system. Nitric Oxide. 2013; 35: 175-85.

[28]. Bauer PM, Buga GM and Ignarro LJ. Role of p42/p44 mitogen-activated protein kinase and p21waf1/cip1 in the regulation of vascular smooth muscle cell proliferation by nitric oxide. Proc Natl Acad Sci USA. 2001; 98: 12802-7.

[29]. Ziche M, Morbidelli L and Masini E, et al. Nitric oxide mediates angiogenesis in vivo and endothelial cell growth and migration in vitro promoted by substance P. J Clin Invest. 1994; 94: 2036-44.

[30]. Kubes P, Suzuki M and Granger DN. Nitric oxide: an endogenous modulator of leukocyte adhesion. Proc Natl Acad Sci USA. 1991; 88: 4651-5.

[31]. Coletta C, Papapetropoulos A and Erdelyi K, et al. Hydrogen sulfide and nitric oxide are mutually dependent in the regulation of angiogenesis and endothelium-dependent vasorelaxation. Proc Natl Acad Sci USA. 2012; 109: 9161-6.

[32]. Xu W, Liu LZ and Loizidou M, et al. The role of nitric oxide in cancer. Cell Res. 2002; 12: 311-20.

[33]. Papapetropoulos A, Garcia-Cardena G and Madri JA, et al. Nitric oxide production contributes to the angiogenic properties of vascular endothelial growth factor in human endothelial cells. J Clin Invest. 1997; 100: 3131-9.

[34]. Mallat Z, Benamer H and Hugel B, et al. Elevated levels of shed membrane microparticles with procoagulant potential in the peripheral circulating blood of patients with acute coronary syndromes. Circulation. 2000; 101: 841-3.

[35]. Bernal-Mizrachi L, Jy W and Jimenez JJ, et al. High levels of circulating endothelial microparticles in patients with acute coronary syndromes. Am Heart J. 2003; 145: 962-70.

[36]. Boulanger CM, Scoazec A and Ebrahimian T, et al. Circulating microparticles from patients with myocardial infarction cause endothelial dysfunction. Circulation. 2001; 104: 2649-52.

[37]. Cheow ES, Cheng WC and Lee CN, et al. Plasma-derived Extracellular Vesicles Contain Predictive Biomarkers and Potential Therapeutic Targets for Myocardial Ischemic (MI) Injury. Mol Cell Proteomics. 2016; 15: 2628-40.